

Thermodynamic modeling of Ionic Liquid physical properties

ABSTRACT: This research focused on investigating the thermophysical characteristics of seven selected Ionic Liquids (ILs), specifically [C_n-TEA][TFSI], and on creating predictive models for these properties using three different thermodynamic approaches. The PC-SAFT Equation of State (EoS) was employed to estimate density, the FVT model was applied to forecast dynamic viscosity, and the mPelofsky model was utilized to compute surface tension. To enhance the accuracy of these models, experimental data from three ILs with differing alkyl chain lengths were used. A nonlinear least-squares technique was implemented to adjust the model parameters by minimizing the discrepancies between predicted values and experimental results.

Following this, a generalized function was formulated to link the optimized model parameters with the number of carbon atoms in the cationic alkyl chains of the ILs. This function allowed for the estimation of model parameters for the remaining four ILs. The performance of the models was evaluated using average absolute deviations (AADs%).

The developed models showed strong predictive capability for the thermo-physical properties of the ILs. In the correlation approach, the AADs% were 0.0163 for density, 4.5534 for viscosity, and 0.1731 for surface tension. For the prediction approach, the deviations were somewhat higher at 0.0780% for density, 6.1122% for dynamic viscosity, and 1.2821% for surface tension. These findings suggest that the models are able effectively predict the properties of other ILs within the same chemical family, offering a valuable tool for further studies.

Keywords: PC-SAFT, FVT, Ionic Liquids, Density, Viscosity, Surface Tension.

1. INTRODUCTION

ILs are a distinctive class of salts that have garnered significant interest in recent years due to their exceptional characteristics, such as low volatility, high thermal and electrochemical

stability, and the ability to tailor their properties for specific applications. These features make ILs highly suitable for diverse uses ranging from separation technologies to energy storage and conversion [1]. However, effectively designing and optimizing processes that involve ILs necessitates precise knowledge of their thermo-physical properties—including density, viscosity, and surface tension. In this regard, thermodynamic models based on equations of state (EoSs) have proven to be effective tools for predicting these properties.

While numerous experimental investigations have been carried out to determine the physical properties of various ILs, the sheer number of possible IL combinations and the wide range of operating conditions make theoretical modeling an appealing alternative. As a result, several modeling strategies—particularly EoSs—have proposed to estimate the thermo-physical behavior of ILs [2], offering a way to calculate key thermodynamic properties.

EoS-based models are particularly effective at predicting derivative thermodynamic properties like density [3]. Although only a limited number of such models have been successfully applied so far, they remain powerful instruments in thermodynamic modeling.

Among the available models, associative EoSs such as CPA and SAFT variants have demonstrated superior performance in describing fluid properties. For example, Llovell et al. [4] combined the Friction Theory (FVT) with the sSAFT EoS to estimate the viscosity of n-alkanes and their mixtures, achieving an average absolute deviation (AAD%) of 2.12%.

In a separate study, Akbari and Alavianmehr [5] integrated the square-well model with the Perturbed Hard Truncated Chain (PHTC) EoS to correlate surface tension data for multiple alkanes and refrigerants across varying temperatures, yielding an average relative deviation of 2.46% over 251 data points.

Polishuk [6] used PC-SAFT, GSAFT+cubic, and CPA EoSs to predict thermodynamic properties of selected ILs containing the [TFSI] anion. In another related work [7], he applied the GSAFT+cubic EoS to estimate properties such as density, sound speed, isothermal compressibility, and isotropic compressibility for heavy alkanes/oils and imidazolium ILs.

Diamantonis and Economou [8] employed SAFT and PC-SAFT EoSs to compute thermodynamic properties—such as vapor pressure, liquid density, heat capacity, and sound speed—for gases relevant to CO₂ removal technologies.

Khoshnamvand and Assareh [9] combined the FVT model with the PC-SAFT EoS to estimate the petroleum reservoir fluids viscosity. Their analysis of six real reservoir systems resulted in an AAD% of 9.7%, showing at least a 6% improvement compared to traditional industrial methods.

Golzar et al. [10] utilized two AI-based approaches—Genetic Function Approximation (GFA) and Artificial Neural Networks (ANN)—to estimate the density, viscosity, and surface tension of five ILs of the type [C_n-TEA][TFSI] (where n = 5, 6, 8, 10, 12). The results from their work will serve as reference benchmarks for comparison with those obtained in this study.

Among the many types of ILs, quaternary ammonium salts incorporating the [TFSI] anion demonstrate strong potential across a variety of applications [11], underscoring the importance of accurately estimating their physical properties. Accordingly, this research focuses on applying the PC-SAFT EoS independently and in mixing with the FVT and mPelofsky (mPelofsky) models to obtain the density, viscosity, and surface tension of seven specific ILs: [C_n-TEA][TFSI], where the cation varies as triethyl(pentyl)ammonium ([TEPA]), triethyl(hexyl)ammonium ([TEHXA]), triethyl(heptyl)ammonium ([TEHA]), triethyl(octyl)ammonium ([TEOA]), triethyl(decyl)ammonium ([TEDA]), triethyl(dodecyl)ammonium ([TEDOA]), and triethyl(tetradecyl)ammonium ([TETDA]), all paired with the bis(trifluoromethylsulfonyl)imide ([TFSI]) anion.

2. MODELS

2.1. Perturbed Chain-Statistical Association Fluid Theory (PC-SAFT) EoS

The PC-SAFT model is a thermodynamic EoS widely used to predict the behavior of fluids [12]. It operates on the principle that molecules in a fluid are not independent but interact with one another through statistical associations. This makes the model particularly effective for fluids with strong intermolecular forces, such as polar or associating compounds. The mathematical formulation of the model is given in equations (1) to (4), which incorporate specific parameters that must be calibrated for each associating component to ensure accurate predictions.

$$\tilde{a}^{res} = \tilde{a}^{hc} + \tilde{a}^{disp} + \tilde{a}^{assoc}. \quad (1)$$

$$\tilde{a}^{hc} = m\tilde{a}^{hs} - \sum_i x_i (m_i - 1) \ln g_{ii}^{hs}(\sigma_{ii}) \quad (2)$$

$$\tilde{a}^{disp} = \left(-2\pi\rho I_1 \overline{m^2 \sigma^3} \right) + \left(-\pi\rho m C_1 I_2 \overline{m^2 \sigma^2 \sigma^3} \right) \quad (3)$$

$$a^{assoc.} = \sum_i x_i \sum_{A_j} \left[\ln X_{A_i} - \frac{1}{2} X_{A_i} + \frac{1}{2} \right] \quad (4)$$

As a result, five parameters— m , σ , ϵ , ϵ_{AiBj} , and κ_{AiBj} must be optimized for associating components, whereas non-associating components only require the first three parameters: m , σ , and ϵ . In the case of ILs, the model employs a 2B association scheme, in which the cation acts as the association site acceptor and the anion serves as the donor. Additional information regarding the equation and its parameters is available in a prior study by the author [13].

2.2. The Free Volume Theory (FVT)

The model proposed by Allal et al. (2001) [14], provides a way to determine the dynamic viscosity (η) of dense fluids, such as liquids, using the following relation:

$$\eta = 4.0785 \times 10^{-5} \frac{\sqrt{M_w T}}{v_c^3 \Omega^*} (1 - 0.2756w) + \rho L \frac{\left(E_0 + \frac{PM_w}{\rho} \right)}{\sqrt{3RTM_w}} \exp \left(B \left(\frac{E_0 + \frac{PM_w}{\rho}}{2RT} \right)^{1.5} \right) \quad (5)$$

All necessary details are included in their mentioned published research. The model includes three tunable parameters: L , E_0 , and B , which correspond to the free space parameter of formation, the molecule diffuse barrier energy, and a dimensionless value, respectively. In this method, the density-dependent parameters needed for the FVT model are calculated using the parameters obtained earlier, with the help of the PC-SAFT equation.

2.3. Modified Pelofsky Model

Ghatee et al. [15] adapted Pelofsky's original model [16] to calculate the surface tension (γ) of ionic liquids (ILs). The revised model is presented in the following equation, where C and D are substance-specific constants, and a universal exponent value of 0.3 is used, as proposed by Ghatee et al. [15].

$$\ln \gamma = \ln C + \frac{D}{\eta^\phi} \quad (6)$$

In this section, the dynamic viscosities are estimated using a combinatorial approach, where FVT (together with PC-SAFT EoS) are utilized with the parameters obtained in the previous sections.

2.4. Prediction Function

In this study, a unified power-law function was utilized to estimate the predictive parameters for all the models described above. The function is defined by equation (7), where X_p represents the parameter being predicted, and n_c refers to the number of carbon atoms in the alkyl chain of the cations within the ionic liquids. Furthermore, the fitting parameters α , β , and λ must be determined individually for each specific parameter to ensure accurate predictions.

$$X_p = \alpha (n_c)^\beta + \lambda \quad (7)$$

3. METHODOLOGY AND DATA SETS EMPLOYED

The experimental data for density, dynamic viscosity, and surface tension of ionic liquids (ILs) featuring alkyl chains with 5, 6, 8, 10, and 12 carbon atoms were collected within a temperature range of 298 to 373 K, as documented by Ghatee et al. [11]. This provided a total of sixteen data points for each property per IL. Furthermore, for ILs with alkyl chains consisting of 7 and 14 carbon atoms, the experimental measurements of all three properties were taken from Machanová et al. [17], covering a temperature range of 293 to 363 K. These yielded eight data points per property for those ILs. It should be emphasized that differences in experimental techniques, equipment, and sample purity across the two studies have led to inconsistencies in the reported values for the same IL under similar conditions. These discrepancies may notably affect the reliability of the modeling outcomes.

In the correlation phase, the physical properties of ILs with pentyl, octyl, and dodecyl chains were analyzed to determine the parameters of equation (7). Following this, a predictive approach was applied to ILs with alkyl chains of 6, 7, 10, and 14 carbon atoms.

It is also important to note that during the correlation process, model parameters are fitted using various objective functions, while in the prediction phase, no further parameter adjustments are made instead, previously correlated parameters are used. As a result, higher average absolute

deviations (AADs%) are typically observed in the predicted results compared to those obtained through correlation.

4. RESULTS AND DISCUSSION

4.1. The Pure Component Physical Properties

To utilize the models described in the study, key physical properties including critical temperature (T_c), critical pressure (P_c), critical volume (v_c), and acentric factor (ω) were estimated using the "modified Lydersen-Joback-Reid (mKJR)" method proposed by Valderrama and Robles [18]. Additional details regarding this method are available in earlier publications by the same authors [19, 20]. The results derived from this approach are summarized in **Figure 1**.

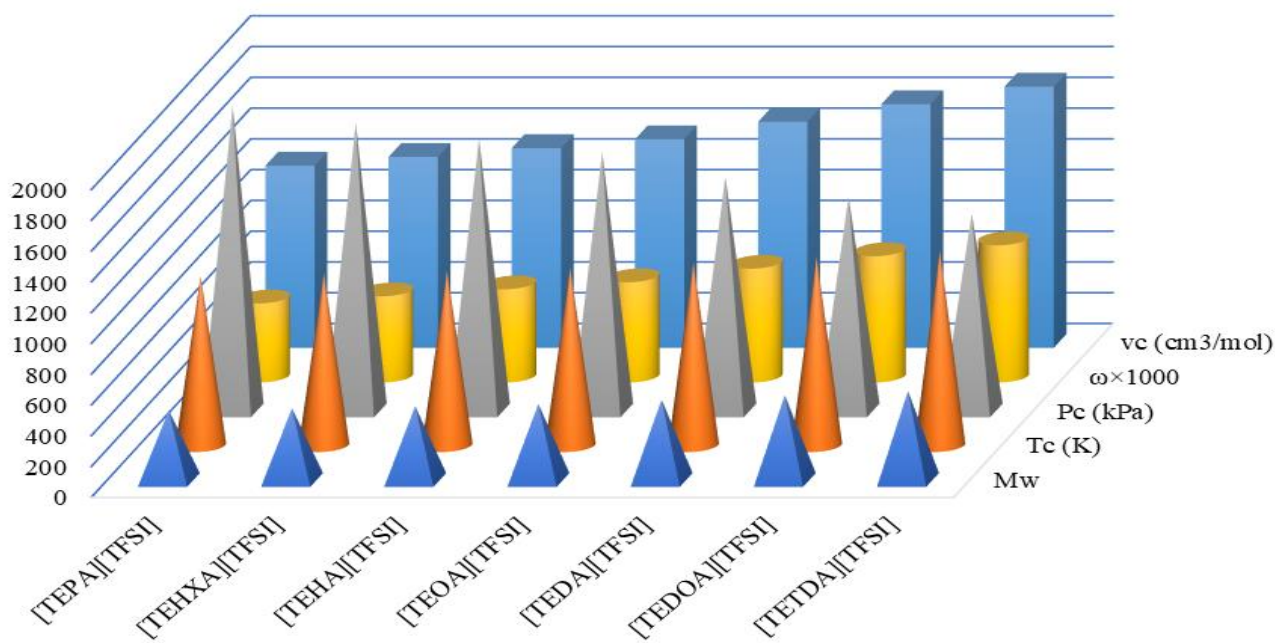


Figure 1. Graphical representation of the physical properties of the ILs.

4.2. The PC-SAFT Pure Components Parameters - Density Calculation

To determine the five optimizable parameters (m , σ , ϵ , $\epsilon^{A_i B_j}$, and $\kappa^{A_i B_j}$) for each associating component, experimental data for liquid densities and vapor pressures are typically used to fit the PC-SAFT model. However, since there were no experimental data available for the investigated ILs, only the liquid density data was utilized to optimize the model parameters. The optimization

was performed using a cost function given in eq. (8), where N represents the total number of data points.

$$AAD(\rho)\% = \frac{100}{N} \sum_i^N \frac{|\rho_i^{exp} - \rho_i^{calc}|}{\rho_i^{exp}} \quad (8)$$

The adjusted parameters and AAD% values for the ionic liquids are presented in **Table 1**. The results show that the PC-SAFT model provides accurate density estimations, with AADs% for all ILs below 0.02.

Table 1. The **CORRELATED** PC-SAFT parameters for the ILs.

Component	m	σ (Å)	ε/k (K)	κ^{AiBj}	ε^{AiBj}/k (K)	N	Ref.	AAD%
[TEPA][TFSI]	2.0228	6.3519	415.5587	0.0080	3057.5349	16	This Work	0.0123
[TEOA][TFSI]	2.0916	6.5764	399.2670	0.0100	2962.7888	16	This Work	0.0196
[TEDOA][TFSI]	2.1385	6.8737	393.6300	0.0084	2963.3000	16	This Work	0.0171
<i>Average AAD%</i>								0.0163

The parameters of equation (7) were determined by correlating the data from **Table 1**, and the resulting calculated values are displayed in **Table 2**.

Table 2. The parameters of Eq. (7) for density **PREDICTION** using PC-SAFT.

X_P	Eq. (7) Coeffs.	[TEHXA][TFSI]	[TEHA][TFSI]	[TEDA][TFSI]	[TETDA][TFSI]
m	α	-0.9690			
	β	-0.9762	2.0555	2.0790	2.1216
	λ	2.2240			
σ (Å)	α	0.0680			
	β	1.0300	6.4263	6.5003	6.7242
	λ	5.9960			
ε/k (K)	α	144.0000			
	β	-0.6333	410.1000	405.7900	397.3000
	λ	363.8000			
κ^{AiBj}	α	3.9820×10^{-7}			
	β	2.8600	0.0080	0.0080	0.0082
	λ	0.0079			

ε^{AiBj}/k (K)	α	-576.0000				
	β	0.1421	3040.0000	3023.5000	2984.0000	2944.9000
	λ	3783.0000				
	Ref.		[11]	[17]	[11]	[17]
	N		16	8	16	8
	AAD(ρ)%		0.1022	0.1786	0.0250	0.0348
	Average AAD%		0.0780			

Tables 2 and 3 demonstrate the strong correlation and predictive power of the model used in this study. As a result, the derived parameters can be effectively utilized to estimate PC-SAFT parameters for other ionic liquids (ILs) within the [Cn-TEA][TFSI] family. Importantly, this means that the density of pure ILs in this group can be predicted without relying on experimental measurements.

It is worth noting that minor discrepancies were expected in the results, particularly for [TEHA][TFSI], due to the use of different data sources for the experimental values. The parameters in equation (7) were derived from data reported in reference [11], but were then applied to predict viscosity values from reference [17]. In essence, the data from reference [17] were used exclusively for validation purposes. Therefore, the resulting predictions serve as evidence of the excellent forecasting ability of the PC-SAFT EoS.

Figure 2 displays the comparison between experimental and calculated densities at various temperatures using the PC-SAFT EoS.

4.3. Dynamic Viscosity Calculation (η)

The FVT model was used to calculate the dynamic viscosity (η) of the ILs. The density values are necessary for this calculation, which were obtained in the previous section. In order to determine the model parameters, the dynamic viscosity data were employed to minimize the objective function shown in eq. (9).

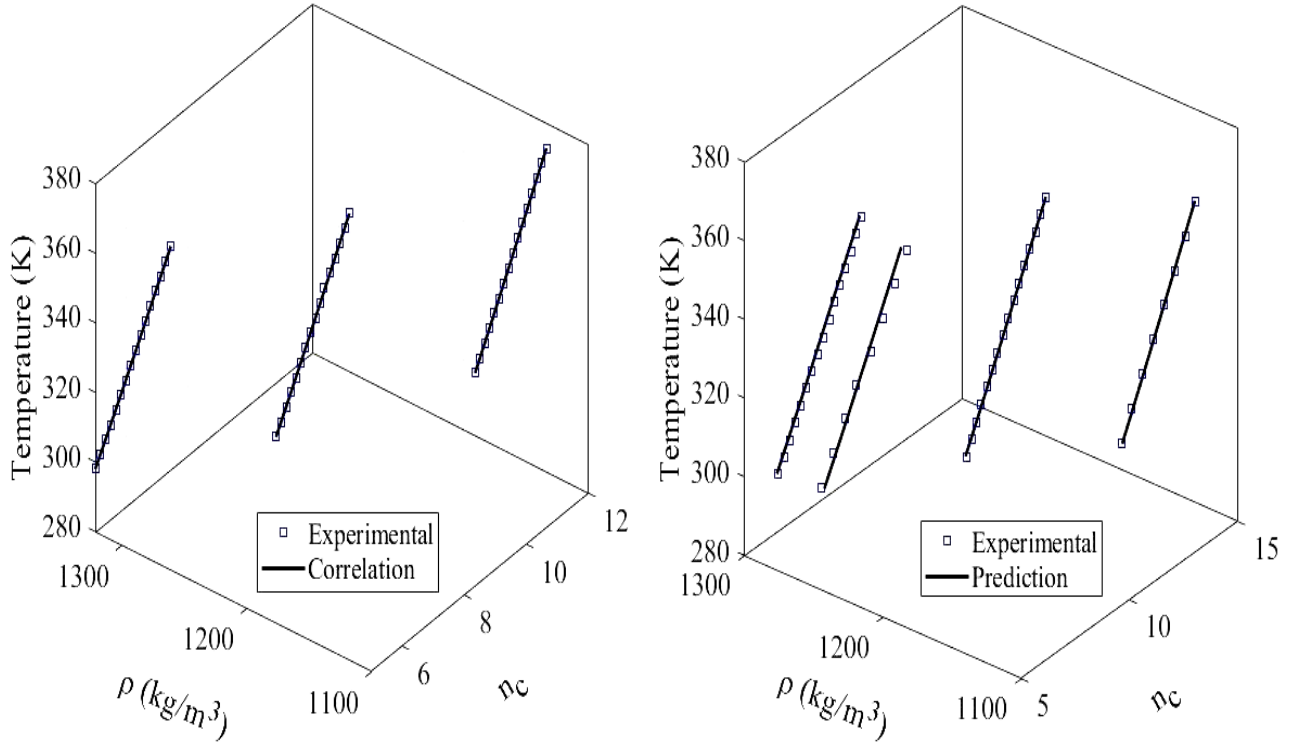


Figure 2. Comparison of Experimental and Calculated Densities at Various Temperatures Using the PC-SAFT Equation of State in Correlation and Prediction Approaches.

$$AAD(\eta)\% = \frac{100}{N} \sum_i^N \frac{|\eta_i^{exp} - \eta_i^{calc}|}{\eta_i^{exp}} \quad (9)$$

The FVT parameters obtained in the correlation scenario are provided in **Table 3**.

Table 3. The **CORRELATED** FVT parameters for the ILs.

Component	$L \times 1010$ (m)	$E0$ (kJ.mol ⁻¹)	B	Ref.	N	$AAD(\eta)\%$	
[TEPA][TFSI]	1.2762	20279.9817	0.2806	[11]	16	4.3722	
[TEOA][TFSI]	0.8344	27240.9242	0.2205	[11]	16	4.2335	
[TEDOA][TFSI]	0.5472	34670.8833	0.1757	[11]	16	5.0544	
Average AAD%						48	4.5534

The results presented in **Table 3** demonstrate a strong correlation ability for the utilized models. By utilizing the values obtained from **Table 3**, we established a correlation between the parameters of Eq. (7). The resultant values have been displayed in **Table 4**.

Table 4. The parameters of Eq. (7) for viscosity **PREDICTION** using FVT.

Xp	Eq. (7) Coeffs.	[TEHXA][TFSI]	[TEHA][TFSI]	[TEDA][TFSI]	[TETDA][TFSI]	
$L \times 10^{10} (m)$	α	4.7690				
	β	-0.6442	1.0887	0.9466	0.6671	0.4563
	λ	-0.4149				
$E_0 (kJ.mol^{-1})$	α	12330				
	β	0.4877	22802	25109	31160	37919
	λ	-6742				
B	α	0.7089				
	β	-0.3334	0.2561	0.2365	0.1950	0.1601
	λ	-0.1340				
Ref.		[11]	[17]	[11]	[17]	
N		16	16	16	16	
AAD (η) %		4.1674	4.0136	5.0076	11.2600	
Average AAD%		6.1122				

Table 4 highlights the strong predictive capability of the models used in this study. It is important to note that when predicting viscosity, the corresponding density values are also predicted simultaneously. Notably, no experimental data is used in this approach for determining either density or viscosity. Therefore, the results reflect purely predictive outcomes.

Figure 3 compares the experimentally measured viscosities with those calculated using the FVT combined with the PC-SAFT model across various temperatures, illustrating both correlation and prediction cases.

The highest average absolute deviations (AADs%) were observed for the ILs [TEHA][TFSI] due to the use of experimental data from a different source for these compounds. Despite this, the results confirm that the applied models demonstrate strong predictive performance.

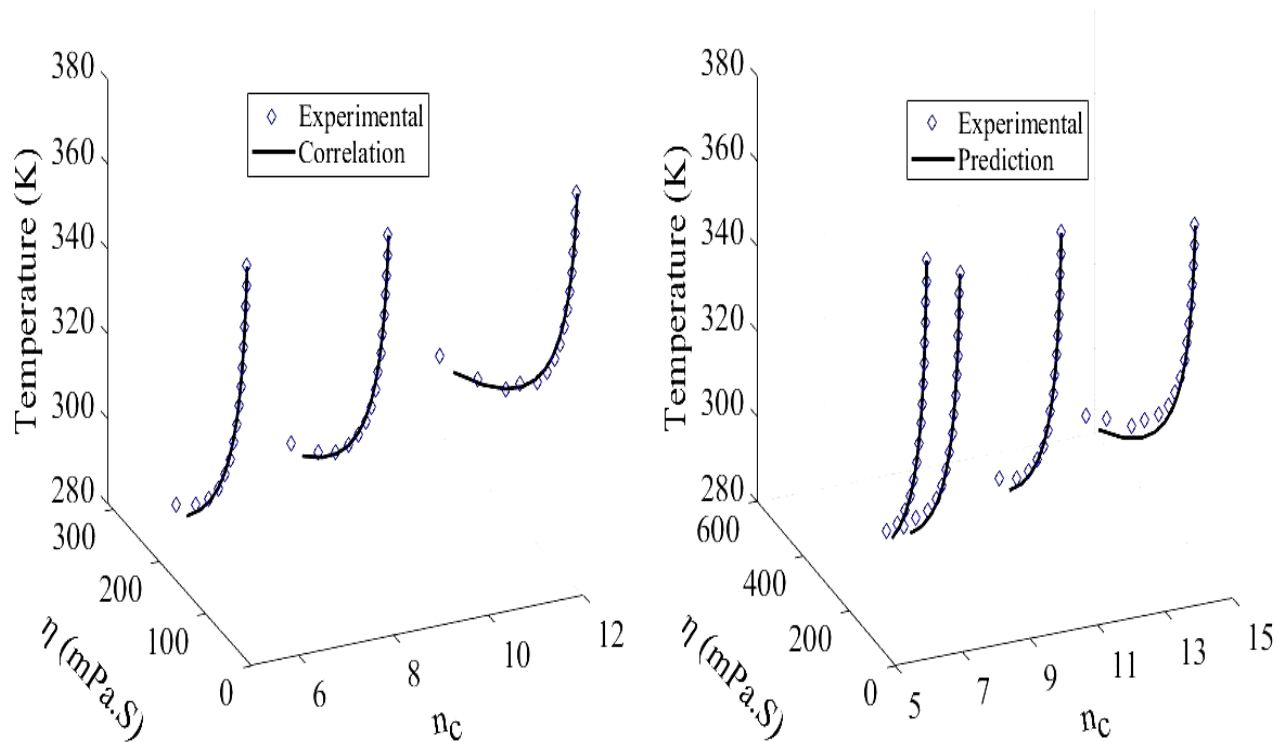


Figure 3. Comparison of Experimental and Predicted Dynamic Viscosities at Various Temperatures Using the FVT Combined with PC-SAFT Model in Correlation and Prediction Approaches.

Table 5 presents a comparison of the average absolute deviation percentages (AADs%) obtained from the Arrhenius, Litovitz, and CPA+FVT models with those from the PC-SAFT+FVT approach for estimating viscosity. It is important to highlight that the Arrhenius and Litovitz models directly fit experimental viscosity data, whereas in the PC-SAFT+FVT method, density values are first predicted using PC-SAFT and then used as input for viscosity calculations via the FVT model. Moreover, the results for the hexyl and decyl ILs are entirely based on predictions, as no experimental data were used in their estimation.

Table 5. A comparison of the viscosities calculated using various models.

Model	ILs					Overall AAD%	Ref.
	[TEPA][TFSI]	[TEHXA][TFSI]	[TEOA][TFSI]	[TEDA][TFSI]	[TEDOA][TFSI]		
Arrhenius	9.80	9.20	9.00	10.60	9.80	9.68	[11]
Litovitz	2.20	3.20	0.98	8.80	1.90	3.42	[11]
CPA +FVT	4.27	8.32	4.11	4.59	4.97	5.25	[19]
PC-SAFT +FVT	4.37	4.17	4.23	5.01	5.05	4.57	This Work

As evident, the new results demonstrate improved accuracies and higher predictive capabilities.

4.4. Surface Tension Calculation (γ)

To compute the surface tension using the modified Pelofsky (mPelofsky) model [15], dynamic viscosity values are required as input. Therefore, the viscosities calculated in the previous section are used for this purpose. However, since there is a lack of experimental surface tension data for ionic liquids (ILs) with alkyl chains containing 7 and 14 carbon atoms, these ILs are excluded from analysis in this section. Experimental data for the remaining ILs were taken from [11].

For model parameter optimization, the following objective function must be minimized:

$$AAD(\gamma)\% = \frac{100}{N} \sum_i^N \frac{|\gamma_i^{exp} - \gamma_i^{calc}|}{\gamma_i^{exp}} \quad (10)$$

Table 6 presents the mPelofsky model parameters obtained in the correlation scenario, aiming to optimize the model's parameters.

Table 6. The mPelofsky model parameters obtained through correlation for the ILs.

Component	$\ln(C (mJ.m^{-2}))$	D	Ref.	N	$AAD(\gamma)\%$
[TEPA][TFSI]	3.7033	-0.5649	[11]	16	0.0711
[TEOA][TFSI]	3.6410	-0.7164	[11]	16	0.1934
[TEDOA][TFSI]	3.6030	-0.8226	[11]	16	0.2548
Average AAD%				48	0.1731

The correlation results demonstrate a high level of accuracy in estimating the surface tension of the ionic liquids (ILs). Based on these findings, the parameters of Equation (7) were derived, and the resulting values are presented in **Table 7**.

The predicted surface tension values achieved an average absolute deviation percentage (AAD%) of 1.382, indicating the strong predictive performance of the models used. It is important to note that, in the prediction approach, calculated viscosity values were used in place of experimental data, showing that accurate predictions can be made without depending on further experimental inputs.

Table 7. The parameters of Eq. (7) for surface tensions **PREDICTION** using mPelofsky model.

X_P	Eq. (7) Coeffs.	[TEHXA][TFSI]	[TEDA][TFSI]
$\ln(C \text{ (mJ.m}^{-2}\text{)})$	α	0.7117	
	β	-0.7807	3.6767
	λ	3.5010	3.6189
D	α	1.6270	
	β	-0.4754	-0.6279
	λ	-1.3220	-0.7775
Ref.		[11]	[11]
N		16	16
$AAD \text{ } (\gamma) \%$		1.8873	0.6768
Average AAD%			1.2821

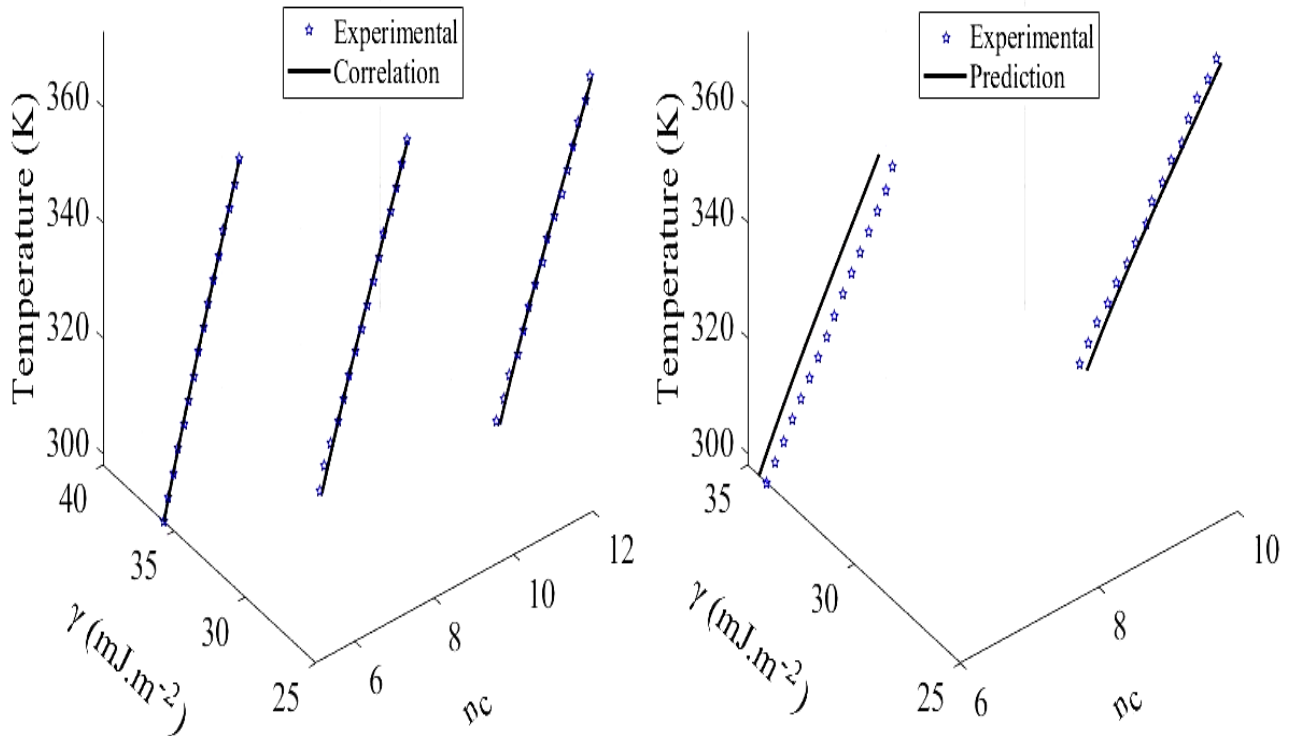


Figure 4. Experimental vs. calculated surface tensions (γ) in different temperatures using the mPelofsky+FVT+ PC-SAFT model in CORRELATION and PREDICTION scenarios.

Figure 4 displays the experimental and calculated surface tension (γ) values at various temperatures using the mPelofsky + FVT + PC-SAFT model, illustrating both correlation and prediction scenarios.

4.5. Comparison with Artificial Intelligence-Based Models

Table 8 provides a comparison of the overall average absolute deviation percentages (AADs%) for density, viscosity, and surface tension obtained in this study with those predicted by established artificial intelligence-based models, namely GFA and ANN. Although the data sets used across these models may vary slightly, a general comparison remains meaningful. The results clearly highlight the effectiveness and accuracy of the modeling approaches employed in this research.

Table 8. A comparison of the overall AADs% for properties estimation using various models.

<i>Model</i> <i>Approach</i>	AADs% for Density				AADs% for Viscosity				AADs% for Surface Tension			
	GFA	ANN	CPA	PC-SAFT	GFA	ANN	CPA +FVT	PC-SAFT +FVT	GFA	ANN	CPA +FVT+ mPelofsky	PC-SAFT +FVT+ mPelofsky
CORRELATION	0.69	0.04	0.02	0.0163	67.72	4.20	4.45	4.5534	0.49	0.34	0.16	0.1731
PREDICTION	0.81	0.04	0.67	0.0780	139.51	6.60	6.46	6.1122	0.45	0.38	1.38	1.2821
Ref.	[10]	[10]	[19]	This Work	[10]	[10]	[19]	This Work	[10]	[10]	[19]	This Work

5. CONCLUSIONS

This study aimed to establish correlations and make predictions for the density, dynamic viscosity, and surface tension of seven ionic liquids (ILs) belonging to the $[C_n\text{-TEA}][\text{TFSI}]$ family, which vary in the number of carbon atoms (5, 6, 7, 8, 10, 12, and 14) in their cationic alkyl chains. A correlation-based analysis was performed on three ILs containing pentyl, octyl, and dodecyl chains, while the remaining ILs were assessed using a predictive approach.

The PC-SAFT equation of state (EoS) was employed to estimate liquid density, yielding average absolute deviations (AAD%) of 0.0163 for the correlation case and 0.0780 for the prediction case. Additionally, the FVT model combined with PC-SAFT was used to calculate dynamic viscosities, and the mPelofsky method integrated with FVT and PC-SAFT was applied for

surface tension estimation. The overall AAD% values were found to be 4.5534 for viscosity in the correlation approach and 6.1122 in the prediction scenario, while for surface tension, they were 0.1731 and 1.2821, respectively.

It is important to note that the model parameters were calibrated using experimental data from ILs with pentyl, octyl, and dodecyl chains from one dataset. These optimized parameters were then used to predict the thermophysical properties of ILs with heptyl and tetradecyl chains from a different dataset.

Finally, a preliminary comparison was made between the results of this study and those obtained using AI-based models. The findings indicate that the models used here perform well in both correlation and prediction tasks. This suggests that it is feasible to reliably estimate the properties of other ILs within this family under various conditions with reasonable accuracy.

List of symbols and abbreviations

AAD	Average Absolute
α	Fitting Parameter in Equation (7)
B	Dimensionless Constant in the FVT Model
β	Fitting Parameter in Equation (7)
λ	Fitting Parameter in Equation (7)
C, D	Parameters of the mPelofsky Model
E_0	Molecular Diffusion Barrier Energy
k	Boltzmann's Constant (1.38066×10^{-23} J/K)
L	Free Space Formation Parameter (m)
m	Number of Molecular Segments
M_w	Molecular Weight
N	Number of Data Points
P	Total Pressure
X_P	Predicted
P_C	Critical Pressure
R	Universal Gas Constant
T	Absolute Temperature
T_C	Critical Temperature
T_r	Reduced Temperature
v	Molar Volume
v_C	Critical Volume
w	Acentric Factor
X^{Ai}	Fraction of Unbonded A-Type Sites on Molecule i

Greek letters

Δ^{AiBj}	Association strength
γ	Surface tension (mJ.m ⁻²)
ε^{AB}	Association energy
ε_i	Segment energy
η	Dynamic viscosity (mPa.S)
ζ	Hard chain term parameter
ρ	Density
σ	Temperature-independent diameter (Å)

Superscript

<i>Cal.</i>	Calculated
<i>Exp.</i>	Experimental

REFERENCES

1. A. Afsharpour, *Petroleum Science and Technology* 37 (14), 1648 (2019) doi:10.1080/10916466.2019.1602633
2. L.F. Vega, O. Vilaseca, F. Llovell, J.S. Andreu, *Fluid Phase Equilibria* 294 (1), 15 (2010) doi: <https://doi.org/10.1016/j.fluid.2010.02.006>
3. J. Greogorowicz, J.P. O'Connell, C.J. Peters, *Fluid Phase Equilibria* 116 (1), 94 (1996) doi:[https://doi.org/10.1016/0378-3812\(95\)02876-5](https://doi.org/10.1016/0378-3812(95)02876-5)
4. F. Llovell, R.M. Marcos, L.F. Vega, *The Journal of Physical Chemistry B* 117 (27), 8159 (2013) doi:10.1021/jp401307t
5. F. Akbari, M.M. Alavianmehr, *Physics and Chemistry of Liquids* 58 (4), 516 (2020) doi:10.1080/00319104.2019.1616192
6. I. Polishuk, *J Phys Chem A* 117 (10), 2223 (2013) doi:10.1021/jp310115p
7. I. Polishuk, *The Journal of Supercritical Fluids* 67, 94 (2012) doi: <https://doi.org/10.1016/j.supflu.2012.02.009>
8. N.I. Diamantonis, I.G. Economou, *Energy & Fuels* 25 (7), 3334 (2011) doi:10.1021/ef200387p
9. Y. Khoshnamvand, M. Assareh, *International Journal of Thermophysics* 39 (4), 54 (2018) doi:10.1007/s10765-018-2377-0
10. K. Golzar, S. Amjad-Iranagh, H. Modarress, *Journal of Dispersion Science and Technology* 35 (12), 1809 (2014) doi:10.1080/01932691.2013.879533

11. Mohammad Hadi Ghatee, Maryam Bahrami, N. Khanjari, *Journal of Chemical Thermodynamics* 65, 10 (2013) doi:10.1016/j.jct.2013.05.031
12. J. Gross, G. Sadowski, *Industrial & Engineering Chemistry Research* 40 (4), 1244 (2001) doi:10.1021/ie0003887
13. A. Afsharpour, S.H. Esmaeli-Faraj, *Korean Journal of Chemical Engineering* 39 (6), 1576 (2022) doi:10.1007/s11814-022-1072-9
14. A. Allal, M. Moha-ouchane, C. Boned, *Physics and Chemistry of Liquids* 39 (1), 1 (2001) doi:10.1080/00319100108030323
15. M.H. Ghatee, M. Zare, A.R. Zolghadr, F. Moosavi, *Fluid Phase Equilibria* 291 (2), 188 (2010) doi: <https://doi.org/10.1016/j.fluid.2010.01.010>
16. A.H. Pelofsky, *Journal of Chemical & Engineering Data* 11 (3), 394 (1966) doi:10.1021/je60030a031
17. K. Machanová, A. Boisset, Z. Sedláková, M. Anouti, M. Bendová, J. Jacquemin, *Journal of Chemical & Engineering Data* 57 (8), 2227 (2012) doi: 10.1021/je300108z
18. J.O. Valderrama, P.A. Robles, *Industrial & Engineering Chemistry Research* 46 (4), 1338 (2007) doi:10.1021/ie0603058
19. A. Afsharpour, *Iranian Journal of Chemistry and Chemical Engineering*, (2023) doi:10.30492/ijcce.2023.1978386.5754
20. A. Afsharpour, *Journal of Molecular Liquids* 324, 114684 (2021) doi: <https://doi.org/10.1016/j.molliq.2020.114684>